WATER RESEARCH 43 (2009) 1700–1710

Available at www.sciencedirect.com

ScienceDirect

journal homepage: www.elsevier.com/locate/watres

Effect of hypolimnetic oxygenation on oxygen depletion rates in two water-supply reservoirs

Paul A. Gantzer[1], *Lee D. Bryant*[2], *John C. Little**

Department of Civil and Environmental Engineering, 418 Durham Hall (0246), Virginia Tech, Blacksburg, VA 24061, USA

ARTICLE INFO

Article history:
Received 12 May 2008
Received in revised form
9 December 2008
Accepted 27 December 2008
Published online 19 January 2009

Keywords:
Anoxia
Diffuser
Hypolimnion
Bubble plume
Oxygenation

ABSTRACT

Oxygenation systems, such as bubble-plume diffusers, are used to improve water quality by replenishing dissolved oxygen (DO) in the hypolimnia of water-supply reservoirs. The diffusers induce circulation and mixing, which helps distribute DO throughout the hypolimnion. Mixing, however, has also been observed to increase hypolimnetic oxygen demand (HOD) during system operation, thus accelerating oxygen depletion. Two water-supply reservoirs (Spring Hollow Reservoir (SHR) and Carvins Cove Reservoir (CCR)) that employ linear bubble-plume diffusers were studied to quantify diffuser effects on HOD. A recently validated plume model was used to predict oxygen addition rates. The results were used together with observed oxygen accumulation rates to evaluate HOD over a wide range of applied gas flow rates. Plume-induced mixing correlated well with applied gas flow rate and was observed to increase HOD. Linear relationships between applied gas flow rate and HOD were found for both SHR and CCR. HOD was also observed to be independent of bulk hypolimnion oxygen concentration, indicating that HOD is controlled by induced mixing. Despite transient increases in HOD, oxygenation caused an overall decrease in background HOD, as well as a decrease in induced HOD during diffuser operation, over several years. This suggests that the residual or background oxygen demand decreases from one year to the next. Despite diffuser-induced increases in HOD, hypolimnetic oxygenation remains a viable method for replenishing DO in thermally-stratified water-supply reservoirs such as SHR and CCR.

1. Introduction

Oxygen-consuming processes that occur naturally in lakes and reservoirs include oxidation of reduced chemical species (Zaw and Chiswell, 1999; Matthews and Effler, 2006a), algal and aquatic respiration (Nakamura and Stefan, 1994) and aerobic decomposition of organic matter (Mackenthun and Stefan, 1998; Moore, 2003; Higashino and Stefan, 2005; Matthews and Effler, 2006a). Lakes in temperate climates undergo seasonal stratification, creating a warmer, less-dense epilimion, a transitionary thermocline or metalimnion, and a colder, more-dense hypolimnion at the top, middle and bottom, respectively (Wetzel, 1975). The density gradient limits oxygen transfer from the surface to the lower hypolimnetic water (Mackenthun and Stefan, 1998). Depletion of dissolved oxygen (DO) in the hypolimnion is exacerbated as algae, which grow in the photic zone, complete their life cycle and are degraded as they settle through the water column. This settling organic detritus undergoes aerobic decomposition in the presence of DO, which contributes to water column

* *Corresponding author*. Tel.: +1 540 231 8737; fax: +1 540 231 7916.
E-mail addresses: paul.gantzer@gmail.com (P.A. Gantzer), lebryan1@vt.edu (L.D. Bryant), jcl@vt.edu (J.C. Little).
[1] Tel.: +1 206 999 1878.
[2] Tel.: +1 540 231 8737; fax: +1 540 231 7916.

0043-1354/$ – see front matter
doi:10.1016/j.watres.2008.12.053

oxygen demand (WOD). Incompletely oxidized detritus settles through the hypolimnion and accumulates on the bottom, becoming incorporated into the sediment and contributing to sediment oxygen demand (SOD) (Higashino and Stefan, 2005; Matthews and Effler, 2006b; Beutel et al., 2007). The net effect of both WOD and SOD in the hypolimnion is an overall hypolimnetic oxygen demand (HOD) (Nakamura and Stefan, 1994; Moore et al., 1996; Beutel et al., 2007). HOD can cause anoxic conditions by completely depleting oxygen in the hypolimnion if the HOD exceeds the amount of DO available in the hypolimnion at the beginning of the stratified period (Burris et al., 2002; Moore, 2003; Matthews and Effler, 2006a; Singleton and Little, 2006; Beutel et al., 2007). Anoxic conditions result in a shift in redox potential as decomposition of organic detritus continues, using other terminal electron acceptors with lower available energy than oxygen (Madigan et al., 2003). This results in the reduction of oxidized compounds (e.g., Manganese (Mn) oxides) and subsequent release of soluble, reduced species (e.g., Mn^{2+}) from the sediment to the hypolimnetic water. Longer periods of anoxia result in more significant deterioration of water quality as reduced species continue to diffuse out of the sediment and enter the hypolimnion (McGinnis and Little, 2002; Matthews and Effler, 2006a).

Several methods are employed to increase hypolimnion oxygen concentrations (Beutel and Horne, 1999; Singleton and Little, 2006). In this study, for simplicity, aeration will refer to systems using compressed air and oxygenation to those using pure oxygen, whether it is supplied from stored bulk liquid or generated on-site. Although these systems are designed to replenish oxygen in the hypolimnion, higher rates of oxygen depletion during periods of aeration or oxygenation are frequently observed. For example, aeration studies have shown that HOD was: (1) 10 times higher in an aerated hypolimnion compared to a non-aerated hypolimnion (Ashley, 1981); (2) approximately double pre-aeration demand in Medical Lake, Washington (Soltero et al., 1994); and (3) observed to increase three to four times during aeration (Lorenzen and Fast, 1977; Moore et al., 1996). Increased oxygen consumption resulting from hypolimnetic aeration or oxygenation has been designated ''induced oxygen demand'' (Beutel, 2003) and is hypothesized to result from both (1) increased SOD (Moore, 2003; Beutel et al., 2007) and (2) increased WOD (Ashley, 1983).

Factors affecting SOD have been extensively studied in laboratory-incubated sediment samples (Moore et al., 1996; Mackenthun and Stefan, 1998; Moore, 2003; Beutel et al., 2007) and using in-situ SOD chambers (Davis et al., 1987). Researchers have investigated the effect of surficial versus deep sediments (Matthews and Effler, 2006b), a multi-layered diffusive boundary layer (DBL) above the sediment–water interface (SWI) (Mackenthun and Stefan, 1998), variations between laminar and turbulent boundaries at the SWI (Mackenthun and Stefan, 1998; Moore, 2003) and have shown that changes in SOD are directly related to water velocities over the sediment (Jorgensen and Revsbech, 1985; Mackenthun and Stefan, 1998; Moore, 2003; Beutel et al., 2007). Although useful for gaining theoretical understanding, small-scale laboratory measurements are not representative of actual reservoir or lake conditions, nor do SOD chambers emulate hydrodynamic conditions at the SWI. Furthermore, oxygenation systems do not necessarily affect the entire sediment surface area (Moore et al., 1996), which emphasizes the importance of analyzing these systems on a basin-wide scale. In addition to questions regarding induced HOD, there are also arguments on whether, after several years of aeration or oxygenation, HOD may in fact *decrease* as the systems more completely satisfy oxygen demand (both WOD and SOD) (McQueen and Lean, 1984; Matinvesi, 1996; Moore et al., 1996; Matthews and Effler, 2006b) thus reducing the ''carry-over'' of latent demand from one year to the next. No comprehensive studies of induced HOD and the potential long-term decrease in HOD have been published to date. In this research, a detailed analysis of two full-scale linear bubble-plume oxygenation systems, located in two different water-supply reservoirs and operated over a wide range of applied gas flow rates, is performed. Our objectives are to investigate: (1) induced HOD as a function of gas flow rate showing the effect of (a) plume-induced mixing and (b) oxygen concentration in the bulk hypolimnetic water; and (2) the long-term reduction of both background and diffuser-induced HOD.

2. Materials and methods

2.1. Study sites

Spring Hollow Reservoir (SHR) (Fig. 1) and Carvins Cove Reservoir (CCR) (Fig. 2) are water-supply reservoirs for the City of Roanoke and surrounding counties, located on private, heavily-forested watersheds in southwestern Virginia, USA. SHR is a pump-storage, side-stream reservoir, supplied with water drawn from the Roanoke River. CCR is supplied by two natural tributaries that flow from agriculturally-dominated lands and two creeks from an adjoining watershed that are routed through diversion tunnels. Linear bubble-plume diffusers, using pure oxygen generated by vaporizing stored liquid, have been installed in both reservoirs. The goal of oxygenation is to improve raw water quality during summer stratification by: (1) increasing and maintaining oxygen levels throughout the hypolimnion as well as in the upper layers of the sediment; (2) minimizing transport of soluble chemical species from the sediment to the bulk water and subsequently reducing chemical demand during the treatment process; and (3) controlling long-term eutrophication by reducing internal phosphorous loading. Oxygenation in both reservoirs has maintained bulk hypolimion oxygen levels in excess of 7 mg l^{-1}, measurable oxygen in the upper layers of the sediment (Bryant et al., in preparation), and reduced levels of soluble Fe^{2+} and Mn^{2+} in the bulk water (Gantzer et al., this work).

SHR and CCR are quite different in terms of reservoir characteristics allowing oxygenation to be studied under dissimilar conditions. The characteristics of both reservoirs and their respective oxygenation systems are summarized in Table 1. While the morphology and depth of SHR tend to shield the hypolimnion from turbulence caused by wind-induced mixing, CCR is shallower and more susceptible to wind-driven effects.

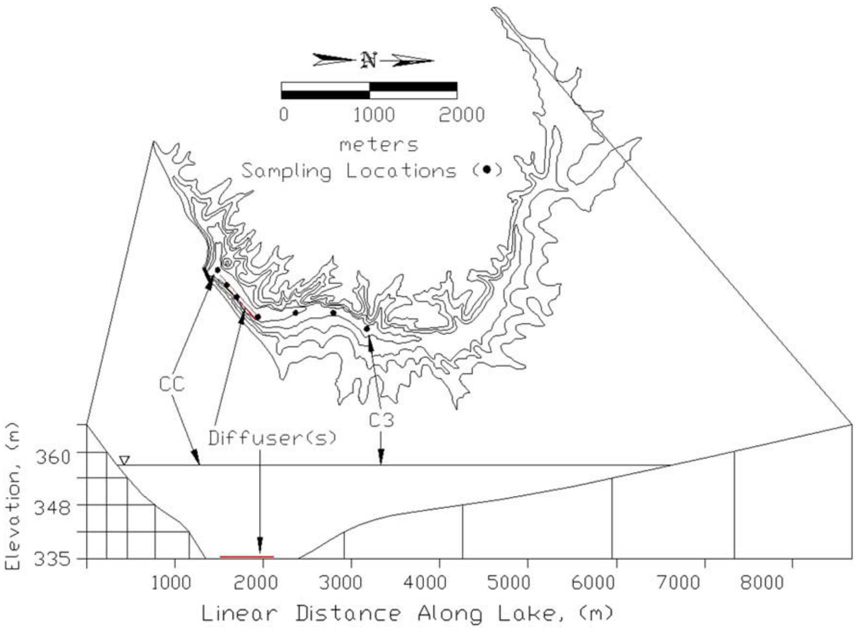

Fig. 1 – Bathymetry, bottom profile, diffuser locations, and sampling stations in Carvins Cove Reservoir.

2.2. *Data collection*

A Seabird Electronics SBE 19plus (4 Hz sampling rate) high-resolution profiler (CTD) was used to collect conductivity, temperature and dissolved oxygen profiles in both reservoirs. The oxygen probe on the CTD has a response time of 1.4 s at 20 °C, allowing data to be collected at 0.1-m increments. A Hydrolab DataSonde 4a multiprobe was used in conjunction with the CTD to obtain profiles at a lower vertical resolution of 0.5 m.

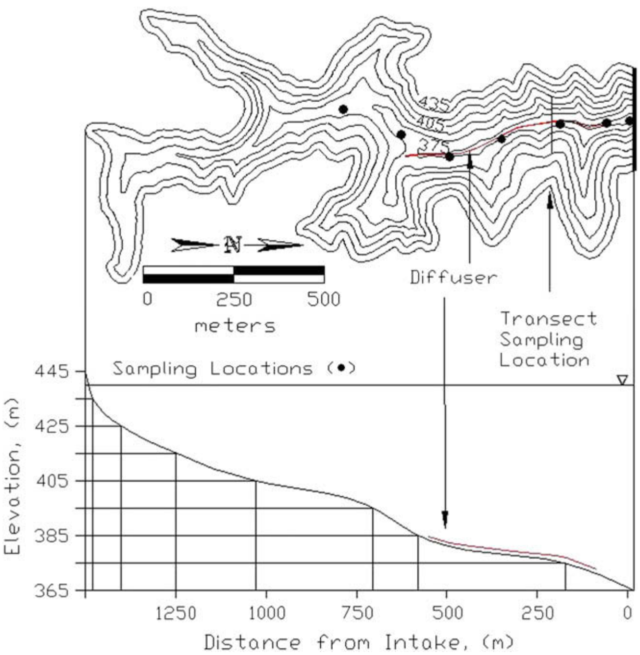

Fig. 2 – Bathymetry, bottom profile, diffuser location, and sampling stations in Spring Hollow Reservoir.

Data collection began in early spring once weather conditions allowed the reservoirs to become accessible and continued through destratification. SHR and CCR begin to stratify in April, although the thermal structure typically does not fully stabilize until May. CCR destratifies in early November while SHR, being deeper, often remains stratified through January. Water column profiles were collected during stratified periods on an average of 36 days per year in CCR (from 2004 to 2007) and 38 days per year in SHR (from 2003 to 2008), yielding a total of over 4800 individual profiles. Profiles were collected weekly during stratification before diffuser operation and at an increased frequency during periods of diffuser operation.

Water column profiles were collected on a longitudinal transect at six and seven locations in SHR and CCR,

Table 1 – Reservoir and oxygenation system characteristics for Spring Hollow Reservoir and Carvins Cove Reservoir.

Parameter	Spring Hollow Reservoir	Carvins Cove Reservoir
Max depth	62 m (200 ft)	21.3 m (70 ft)
Surface area	0.61 km^2 (150 acres)	2.5 km^2 (1100 acres)
Volume	13×10^6 m^3 (3.4×10^9 gal)	24×10^6 m^3 (6.2×10^9 gal)
Hypolimnion volume (% total volume)	15	25
Oxygen demand (kg day^{-1})	~50	~430
Side slopes	1.5–2:1	8–20:1
Diffuser length	620 m (2000 ft)	1250 m (4000 ft)
Design flow rate	34 NCMH (20 SCFM)	68 NCMH (40 SCFM)
Design O_2 addition (kg day^{-1})	~1000	~2100
O_2 transfer efficiency (%)	95–98	80–85

respectively (Figs. 1 and 2). These locations span the entire hypolimnion and include locations upstream, downstream, and in the immediate vicinity of the diffusers. Lateral transects of water column profiles were also collected covering 60 and 80 locations across the diffuser lines in SHR and CCR, respectively, to more accurately characterize the bubble plumes produced by the oxygenation systems (Singleton et al., 2007).

2.3. *Data analysis*

The water column profiling strategy focused on capturing oxygen conditions in the hypolimnion before, during and after periods of oxygenation. Calculations based on CTD profile data were performed to determine HOD. This was done by first analyzing temperature profiles to determine the boundary between the metalimnion and hypolimnion, and the corresponding hypolimnetic volume. The reservoir was then divided into several sections (based on longitudinal sample locations) and vertical layers (based on sampling depth locations) to determine the oxygen mass associated with the measured oxygen concentrations. Total oxygen mass as well as volume-averaged oxygen concentrations were determined as a function of time. Oxygen mass, average oxygen concentration and hypolimnetic volume during each time period were then used to determine HOD as a function of oxygen mass (HOD_{mass}) and oxygen concentration (HOD_{conc}). This procedure was also used to establish background HOD when the diffuser was not in operation.

During operation, oxygen is added to the water column via a bubble plume. To quantify the effect of the diffuser system on HOD, a previously validated plume model (Singleton et al., 2007) was used to estimate the amount of oxygen added to the hypolimnion. The diffuser-induced HOD was then calculated by determining the difference between the amount of oxygen added (predicted data) and the amount observed in the water column (measured data). Water column temperature profiles were used to determine the rate of hypolimnetic warming, which is indicative of mixing associated with diffuser operation.

2.3.1. *Determining thermocline location*

Following Wetzel (1975), the boundary of the hypolimnion was determined as the point of intersection between lines drawn through the thermocline and bulk hypolimnion temperature profiles. Our approach follows similar work done by Quinlan et al. (2005) which uses the inflection method and includes the lower portion of the metalimnion in the hypolimnion. Energy exchange between the hypolimnion and metalimnion results in downward movement of the thermocline throughout the year (Eckert et al., 2002). The resulting warming of the hypolimnion corresponds with oxygen transfer between these layers (Davis et al., 1987; Eckert et al., 2002) and thus affects the amount of oxygen in the hypolimnion. Defining the hypolimnetic volume as a function of thermocline position and hypolimnion temperature provides a consistent basis for evaluating the effects of diffuser-induced mixing.

2.3.2. *Oxygen content*

Dissolved oxygen profiles of the water column were obtained at six and seven locations along SHR and CCR, respectively. Each reservoir was divided into sections based on the profile locations. CTD profiles collected at increments of 0.1–0.2 m were converted to a uniform 0.1-m grid using linear interpolation between consecutive data points. Each section was divided into 0.1-m layers. This created a section (*x*)–layer (*z*) grid that divided the reservoir into cells. The volume-weighted total mass of oxygen in the hypolimnion was calculated by multiplying the oxygen concentration ($DO_{x,z}$) by the corresponding cell volume ($Vol_{x,z}$) and summing the results for all cells:

$$Mass = \sum_{x=1}^{s} \sum_{z=1}^{n} DO_{x,z} \times Vol_{x,z} \quad (1)$$

where Mass = total volume-weighted oxygen mass (kg), $DO_{x,z}$ = oxygen concentration in section (*x*) and layer (*z*), $Vol_{x,z}$ = cell volume corresponding to section (*x*) and layer (*z*), *s* = number of sections, and *n* = number of layers.

Dividing mass by total volume yields the volume-weighted oxygen concentration, thus normalizing the data for comparison among years and between reservoirs. An analogous approach was used to estimate the metalimnetic oxygen content.

2.3.3. *Hypolimnetic oxygen demand (HOD)*

HOD_{mass} is commonly calculated by dividing the mass differential by the time differential between two consecutive sampling days (Davis et al., 1987) or by plotting hypolimnion oxygen content against time and finding the slope of the regression line through the data (Lorenzen and Fast, 1977). However, closer examination of these methods has revealed that volume fluctuations resulting from thermocline movement (as discussed in Section 2.3.1) can cause variations in results for HOD. To take hypolimnion volume variability into account, two calculation approaches were employed based on the regression method outlined by Lorenzen and Fast (1977) and applied to: (1) oxygen mass, with corrected hypolimnetic volume fluctuations, and (2) oxygen concentration, and multiplying by the averaged hypolimnion volume for specific time periods. Results of the two methods, which had an average error between them of less than 1%, were averaged to determine oxygen depletion (HOD_{mass}) and accumulation rates. Dividing HOD_{mass} by each period's hypolimnion volume results in a volume-averaged hypolimnion oxygen demand based on concentration, HOD_{conc}. The metalimnetic oxygen demand (MOD) was estimated using an analogous approach.

As discussed in Section 3.1, settling organic detritus accumulates in the metalimnion and exerts a disproportionate and localized oxygen demand. The MOD is of interest because detritus settling through the metalimnion subsequently enters the hypolimnion where it may contribute to HOD via both WOD and eventually SOD. An important assumption in calculating MOD (as well as HOD) is that vertical transport of oxygen (from the epilimnion down into the metalimnion, and from the hypolimnion up into the metalimnion) may be neglected. A rough analysis of the oxygen concentration gradients immediately above and below the metalimnion suggested that these combined vertical fluxes were small relative to the calculated MOD.

2.3.4. *Oxygenation and bubble-plume model predictions*

Bubble plumes release oxygen bubbles directly into the hypolimnion in contrast to other oxygen transfer devices (for example, the Speece Cone (Moore, 2003; Singleton and Little, 2006) or air-lift aerator (Burris et al., 2002)) that entrain hypolimnetic water and discharge oxygen-enriched water through an engineered structure. When designed appropriately, bubble-plume diffusers add oxygen to the deep waters of the hypolimnion via a detraining bubble plume that induces circulation and distributes newly-oxygenated water throughout the hypolimnion, while preserving thermal structure (McGinnis et al., 2004; Singleton and Little, 2006; Singleton et al., 2007).

A linear bubble-plume model, validated by Singleton et al. (2007), was used to predict the rate at which oxygen was added to the hypolimnion on each day of operation that data were collected. Input variables for the model are water column profiles (temperature, conductivity and oxygen concentration), gas flow rate, percent oxygen content in the supply gas, initial bubble size and diffuser characteristics (depth, width and length). Model outputs include oxygen addition rate, depth of maximum plume rise (DMPR), equilibrium depth (ED) and the predicted oxygen and temperature profiles within the plume. DMPR is the height within the water column to which the plume water rises before detraining while ED, which does not account for further entrainment into the detraining plume water, is the estimated depth to which the plume water returns (the depth at which the ambient density is equal to that of the detraining plume). The oxygen addition rate predicted by the plume model was compared to hypolimnion accumulation rates to determine HOD_{mass} during periods of diffuser operation.

2.3.5. *Induced HOD*

Induced HOD is calculated by comparing background oxygen depletion rates measured before diffuser operation began with those observed during oxygenation. Depletion rates during oxygenation are calculated from the difference between predicted oxygen addition (plume model output) and observed hypolimnetic oxygen accumulation (water column analysis). The actual addition rate is expected to be relatively constant because (1) flow control was maintained by an Alicat Scientific digital mass flow controller and (2) the bulk oxygen concentration (C_{bulk}) of $\sim$10 mg l^{-1} is much lower than the saturated oxygen concentration (C_{sat}) in the deep water of the hypolimnion at approximately 3 and 7 bar for CCR and SHR, respectively. An increase in the bulk dissolved oxygen concentration of a few milligrams per liter is therefore small relative to the overall concentration driving force ($C_{sat} - C_{bulk}$). Diminished oxygen accumulation rates are thus primarily caused by an increased rate of oxygen consumption.

2.3.6. *Hypolimnetic mixing*

Mixing throughout the water column can occur naturally due to wind-driven processes (Eckert et al., 2002) or artificially due to oxygenation. Natural and artificial mixing in the hypolimnion can cause: (1) increased turbulence in the hypolimnion (Ashley, 1981, 1983); (2) enhanced rates of hypolimnion warming (Soltero et al., 1994; Thomas et al., 1994); (3) increased SOD (Moore et al., 1996; Moore, 2003; Beutel et al., 2007); and (4) a uniform temperature throughout the hypolimnion. Hypolimnetic warming is perhaps the easiest to quantify, and is used to evaluate the effect of diffuser-induced mixing.

2.3.7. *Hypolimnetic warming*

The rate of hypolimnetic warming is calculated using a method similar to that used for oxygen mass (Section 2.3.2). CTD profiles were converted to uniform 0.1-m layers for each section. The resulting section (x)–layer (z) grid divided the reservoir into cells, each with a known temperature. The change in sensible heat for each cell was found by multiplying the temperature difference between sample days ($T_{x,y+1,z} - T_{x,y,z}$) by the corresponding cell mass ($m_{x,y,z}$) and the sensible heat coefficient (c) and then summing over each layer:

$$Q_z = \sum_{x=1}^{s} \sum_{y=1}^{p} m_{x,y,z} \times c \times \left(T_{x,y+1,z} - T_{x,y,z}\right) \tag{2}$$

where Q_z = change in sensible heat of layer (z) (kJ), $m_{x,y,z}$ = water mass for section (x), day (y), at layer (z) (kg), $c = 4.190$ kJ kg^{-1} $^{\circ}C^{-1}$, $T_{x,y,z}$ = cell temperature for section (x), day (y), at layer (z) ($^{\circ}$C), s = number of sections, and p = sample day.

Dividing sensible heat by the number of days during the sample period yields a rate of change of sensible heat for each layer, which is then plotted as a function of elevation. Summing the rate of change of heat over all hypolimnion layers and normalizing by hypolimnion volume generates the total rate of change of heat per unit hypolimnion volume, which is used to evaluate hypolimnetic warming at different applied gas flow rates.

3. Results and discussion

3.1. *Hypolimnetic anoxia*

The oxygenation system in SHR was not operated in 2001, allowing baseline conditions without diffuser operation to be established. The development of hypolimnetic anoxia during this period is revealed in Fig. 3, with dissolved oxygen isopleths created using oxygen profile data collected from a single location at the deepest point in the reservoir. The 12 °C temperature isopleth is also shown, indicating the approximate boundary between the metalimnion and the hypolimnion.

Fig. 3 shows the net effect on the water column of all oxygen-depleting processes (chemical and biological). The evaluation of HOD is based on all oxygen-consuming processes in the hypolimnion and includes WOD, which is primarily caused by detrital decomposition, and SOD, which encompasses biological and chemical processes largely associated with organic matter decomposition (Davis et al., 1987). Fig. 3 shows that HOD is driven by oxygen depletion both at the bottom of the hypolimnion due to SOD and in the hypolimnetic water column due to WOD from settling organic detritus. Additionally, MOD, which is caused by detritus accumulating in the metalimnion, reduces the amount of

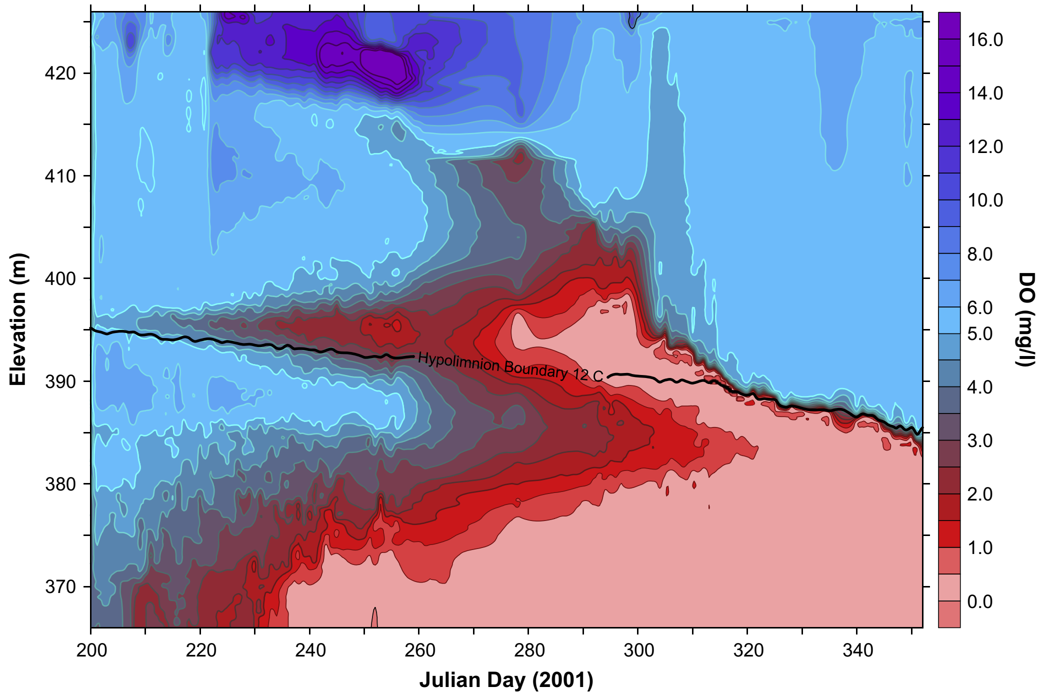

Fig. 3 – Dissolved oxygen isopleths in SHR during summer stratification in 2001, the only year the oxygenation system was not operated. The 12 °C temperature isopleth represents the approximate upper boundary of the hypolimnion.

oxygen available for subsequent detrital degradation. When the accumulated detritus finally settles through the metalimnion into the hypolimnion during the latter part of the summer, this organic material exerts a higher WOD in the hypolimnion, because it has not been degraded to the same extent as that entering the hypolimnion during the earlier part of the summer.

Algal growth in the epilimnion occurred between Julian day 220 and 260 and subsequently exerts MOD as the algae settle and begin to decompose. Detrital buildup in the metalimnion occurs as particle settling velocities decrease due to water density changes as particles sink from warmer to colder water. As an illustration, temperatures in SHR in August are commonly 23 °C in the epilimnion and 5 °C in the hypolimnion. Using Stoke's Law and assuming a particle diameter of 140 μm and a density of 1100 kg m^{-3} (particle size ranges from 20 to 200 μm and densities range from 1030 to 1230 kg m^{-3} (Agusti et al., 1987; Weilenmann et al., 1989)), the settling velocity decreases from about 0.4 to 0.3 m day^{-1} as the particle sinks through the metalimnion. The resulting accumulation of organic material therefore exerts a disproportionate oxygen demand at this depth, which can lead to what is known as a ''metalimnetic minimum'' in oxygen concentration.

Hypoxic conditions in the hypolimnion were observed to progress upwards from the reservoir bottom over time (Fig. 3). This demonstrates the impact that SOD has on oxygen in the hypolimnion, and coincides with the results of Davis et al. (1987) which showed that SOD comprised ~80% of HOD during early stratification.

The decreased oxygen levels in the upper hypolimnion shown in Fig. 3 suggest that the oxygen demand associated with setting detritus (WOD) became noticeable in mid-August (~day 225). Closer examination of Fig. 3 indicates that settling detritus clearly affected hypolimnion oxygen concentrations by early October (~day 260). As the lower hypolimnion is essentially anoxic at this point, the dominant contributor to HOD shifts from SOD to WOD during late stratification, as observed by Davis et al. (1987). Because vertical diffusion of oxygen is insufficient to eliminate the metalimnetic minimum, the only way for oxygen to increase in the metalimnion is if the oxygen-consuming detritus is removed. As the accumulated organic material finally settles through the metalimnion and enters the hypolimnion, the oxygen demand associated with the decomposition of this material shifts from the metalimnion (allowing oxygen to increase in this layer) to the hypolimnion (causing an increase in WOD). SOD at this stage is curtailed by the large volume of anoxic water above the sediment. By the end of October (~day 300), the metalimnion is also anoxic, limiting further detrital decomposition in that region. Organic detritus continues to settle from the anoxic metalimnion into the hypolimnion, which is close to being completely anoxic. The incompletely-oxidized detritus, now undergoing slower anaerobic decomposition, settles to the bottom and becomes incorporated in the surface sediment, from where it can again exert an oxygen demand when oxygen becomes available after the annual overturn.

3.2. *HOD and gas flow rates*

As stated previously, the change in HOD_{mass} prior to the start of diffuser operation represents the background depletion rate. During diffuser operation, HOD_{mass} was calculated as the difference between observed water column accumulation and oxygen addition predicted by the plume model. For example,

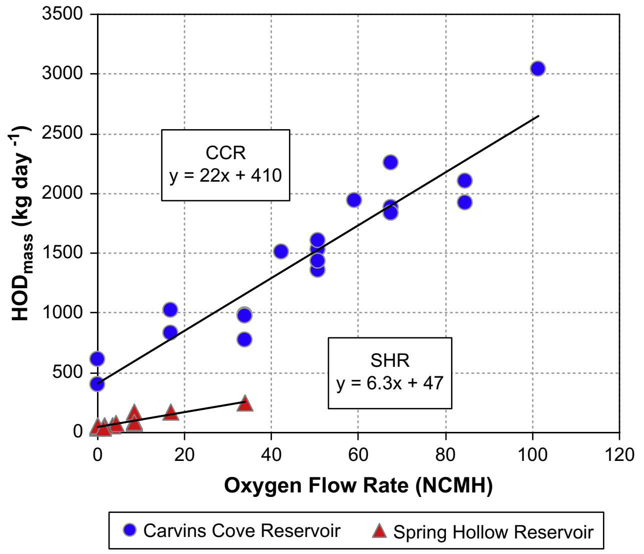

Fig. 4 – Hypolimnetic oxygen demand in Carvins Cove Reservoir and Spring Hollow Reservoir as a function of applied gas flow rate. The y-intercept represents the background HOD_{mass} with zero gas flow.

an 8.5 NCMH (5 SCFM) oxygen flow rate applied to the diffuser in SHR yielded a predicted oxygen addition rate of 266 kg day^{-1}. The observed oxygen accumulation rate in the hypolimnion during this period was 181 kg day^{-1}. The calculated HOD_{mass} during the period was therefore ~85 kg day^{-1}.

The oxygenation systems were operated at gas flow rates ranging from 2 to 50 NCMH (1 to 30 SCFM) and 17 to 102 NCMH (10 to 60 SCFM) in SHR and CCR, respectively. HOD_{mass} and the corresponding applied gas flow rates are plotted in Fig. 4, revealing a linear relationship for both SHR and CCR. The intercept for both regression lines represents the background HOD_{mass} for each reservoir and the corresponding *P*-values for SHR and CCR are 2.0×10^{-6} and 2.3×10^{-11} respectively. The increase in HOD_{mass} above the background represents induced HOD_{mass}. For example, during the initial years following oxygenation at SHR, calculated background HOD_{mass} was observed to be ~50 kg day^{-1}. At 17 NCMH, the HOD_{mass} is ~150 kg day^{-1}; 50 kg day^{-1}due to background depletion and 100 kg day^{-1} induced by operating the diffuser. The same flow rate applied to CCR would yield an induced demand of ~370 kg day^{-1}, with an overall HOD_{mass} of ~790 kg day^{-1}.

To account for the induced oxygen demand associated with the operation of aeration and oxygenation systems, it has been suggested that a factor of safety should be used (Cooke et al., 2005). Results supporting the need for such a safety factor show that the induced demand: (1) is caused by increased SOD (Cooke et al., 2005); (2) ranges from a factor of 1.5 to 4.0 (Soltero et al., 1994; Moore et al., 1996; Prepas et al., 1997; Beutel, 2003); and (3) is dependent on hypolimnion size (Cooke et al., 2005). Our research builds on these results by showing that induced demand: (1) is caused by both SOD and WOD; (2) ranges beyond a factor of 6.0; and (3) is strongly dependent on applied gas flow rate, but is essentially independent of hypolimnion size (as discussed in Section 2.3.3).

Increasing the gas flow rate to the diffuser increases the degree of mixing and the oxygen concentration in the hypolimnion and both of these factors could theoretically increase HOD. Elevated oxygen concentrations increase the driving force for oxygen transfer across the DBL at the SWI, which increases the flux of oxygen into the sediments (Rasmussen and Jorgensen, 1992). Increased turbulence results in a decreased DBL thickness, which would also increase the flux of oxygen into the sediments (Jorgensen and Revsbech, 1985; Mackenthun and Stefan, 1998; Moore, 2003; Beutel et al., 2007). To establish which of these two effects (oxygen concentration versus turbulent mixing) is most significant, we first examined the rate of diffuser-induced hypolimnetic warming caused by the bubble plume and then evaluated the dependence of HOD on bulk water oxygen concentration.

3.3. *Hypolimnetic warming*

Temperature profiles were analyzed during each flow period to determine the rate of hypolimnetic warming. Fig. 5 shows warming rate versus elevation for the range of gas flow rates applied to the SHR diffuser. The data for each period of diffuser operation are truncated at the hypolimnion boundary. Higher rates of warming in the upper hypolimnion indicate warmer water from the metalimnion mixing with the upper hypolimnion. Fig. 5 clearly shows higher warming rates throughout the hypolimnion at higher gas flow rates, confirming the occurrence of plume-induced mixing. A similar effect was observed in CCR, although the data are not shown here.

To more closely relate mixing to gas flow rates, total warming rates per unit hypolimnion volume (kJ m^{-3} day $^{-1}$) were calculated for both SHR and CCR, as shown in Fig. 6. The observed hypolimnetic warming rates in SHR were calculated over a range of applied gas flow rates and over a period of several years (2003–2007). Similar data for CCR (for the years 2005–2007) are also plotted in Fig. 6. The variability in warming

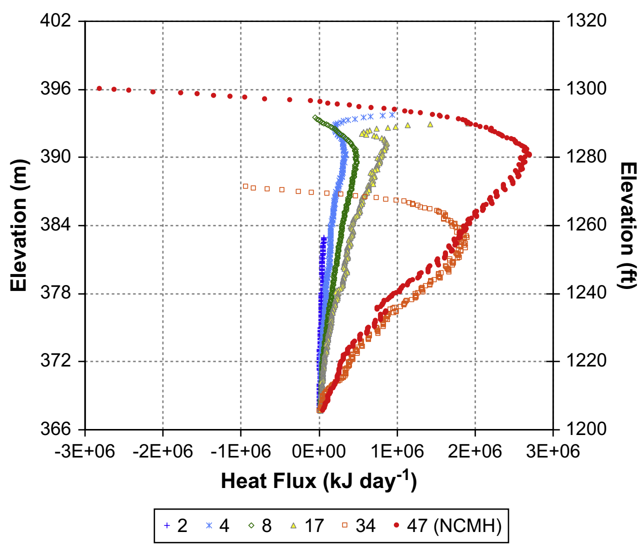

Fig. 5 – Hypolimnetic warming in Spring Hollow Reservoir as a function of elevation and applied gas flow rate, with data cropped off at hypolimnion boundary.

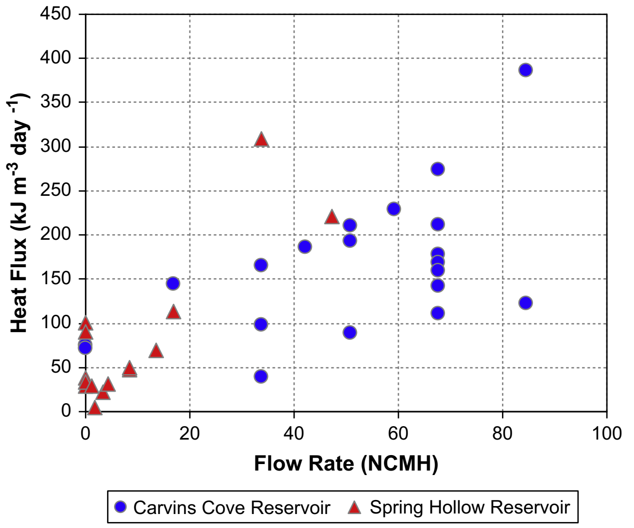

Fig. 6 – Total warming rates per unit hypolimnion volume in Carvins Cove Reservoir and Spring Hollow Reservoir as a function of applied gas flow rate.

rates at similar applied gas flow rates (particularly for CCR) shows that hypolimnetic warming is also affected by external conditions, such as the wind. Despite these weather-related effects, a linear relationship between applied gas flow rate and diffuser-induced mixing is evident in Fig. 6. A regression of the data set yields P-values of 0.0086 and 6.4×10^{-5} for CCR and SHR, respectively. Overall, the relationship between hypolimnetic warming and gas flow rate (Fig. 6) is quite similar to that between HOD_{mass} and gas flow rate (Fig. 4), suggesting

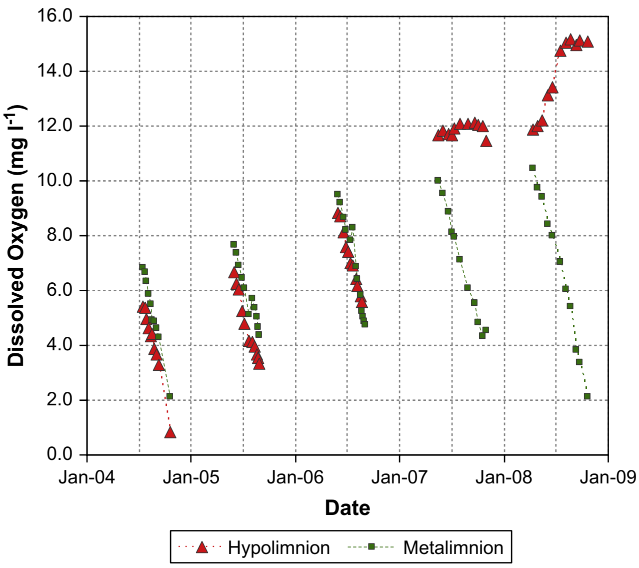

Fig. 7 – Volume-averaged dissolved oxygen concentration in the metalimnion and hypolimnion of Spring Hollow Reservoir. Data show background concentration rates observed before diffuser operation for 2004–2006. Data for 2007 and 2008 correspond to continuous diffuser operation at 1.3 and 0.61 NCMH, respectively.

that mixing induced by the bubble plume is an important contributor to the increase in HOD.

3.4. *Effect of bulk oxygen concentration on HOD*

Mass transfer theory suggests that SOD is regulated by hydrodynamic forces in the water overlying the sediment coupled with the oxygen concentration driving force between the bulk water and the sediment ($C_{bulk} - C_{sed}$) (Jorgensen and Revsbech, 1985). SHR's low background HOD allowed several months of data to be collected before oxygenation was required. The low oxygen demand also provided an opportunity to operate the diffuser at flow rates low enough to minimize induced mixing and the related oxygen demand. Fig. 7 shows volume-averaged oxygen concentration in SHR during summer stratification, but prior to diffuser operation (2004–2006) and during diffuser operation at a low flow rate (2007–2008). The gas flow rate during 2007 and 2008 was only 1.3 NCMH and 0.61 NCMH, respectively. Fig. 7 shows that the initial volume-averaged hypolimnion oxygen concentration increased each year, while the slope of the data (representing HOD_{conc}) is essentially constant. The initial DO and corresponding HOD_{conc} for each year is summarized in Table 2, confirming that the higher bulk DO does not cause an increase in HOD_{conc}.

It has been observed that higher oxygen concentrations can cause increased depletion rates (Jorgensen and Revsbech, 1985). Our results, however, show that despite maintaining an elevated oxygen concentration in the hypolimnion, the depletion rate did not increase. To further evaluate these results, we performed the same analysis on the metalimnion data, which show the same trend to that observed in the hypolimnion, as shown in Fig. 7. Increased oxygen concentrations in the bulk water did not result in elevated depletion rates in either hypolimnion or metalimnion. In fact, the opposite was observed as HOD_{conc} tended to decrease over time. Overall, Table 2 shows that the individual depletion rates (HOD_{conc} and MOD_{conc}), as well as the combined depletion rate, decreased in SHR between 2003 and 2008. It can therefore be concluded that induced HOD is primarily caused by mixing. Relatively constant background depletion rates shown in Fig. 8 and Table 2 for 2004–2006 further suggest that HOD is a zero-order process with respect to oxygen concentration. Additionally, the higher initial concentrations for 2004–2006 (see Fig. 7) have no apparent effect on the subsequent depletion rate, again suggesting a zero-order consumption process. In summary, Fig. 8 shows that (1) the overall WOD from the metalimnion and the hypolimnion has decreased with continued oxygenation and (2) the WOD appears to shift from the hypolimnion to the metalimnion. These changes in WOD during diffuser operation are therefore not related to oxygen concentration, but are likely controlled by mechanisms related to increased turbulence, including the residence time of settling organic matter in the hypolimnion.

3.5. *Effective depth*

Ashley (1983) suggested that an observed increase in oxygen demand in Black Lake, British Columbia was a result of hypolimnetic aeration increasing the "effective depth" of the

Table 2 – Initial volume-averaged oxygen concentrations and subsequent oxygen depletion rates in the hypolimnion and metalimnion of Spring Hollow Reservoir.

Date	Hypolimnion		Metalimnion		Total
	Initial DO ($mg\ l^{-1}$)	HOD_{conc} depletion rate ($mg\ l^{-1}\ day^{-1}$)	Initial DO ($mg\ l^{-1}$)	MOD_{conc} depletion rate ($mg\ l^{-1}\ day^{-1}$)	Depletion rate ($mg\ l^{-1}\ day^{-1}$)
2003	12.7	0.047	8.1	0.047	0.094
2004	5.4	0.046	6.8	0.050	0.096
2005	6.7	0.036	7.6	0.052	0.088
2006	8.8	0.039	9.5	0.057	0.096
2007	11.9	0.032	10.9	0.037	0.069
2008	15.0	0.014	10.4	0.043	0.057

hypolimnion. The idea is that settling material is stirred up, prolonging the residence time of the organic detritus in the aerobic decomposition zone and subsequently "extending" the depth of the hypolimnion through which this material must settle. This was evaluated in CCR by deploying sediment traps. The traps were positioned 2 m above the sediment at locations directly over different points of the diffuser (sample locations CC, CB and CE) and at locations 600 and 1150 m away from the diffuser (sample locations C2 and C3, respectively). The sediment traps were monitored bi-weekly for total solids between September and October, 2006. The results from September 25, October 2 and October 20 show increased accumulation in the sediment traps directly over the diffuser (17,900, 17,700 and 24,600 $mg\ l^{-1}$) compared to those positioned further away (6400, 7300 and 4700 $mg\ l^{-1}$). These results support the effective depth concept by suggesting that particles in the vicinity of the diffuser remain suspended in the water column due to mixing induced by the bubble plume. Increasing the period of time that organic matter remains suspended in the water column allows more complete oxidation, which leads to an increase in WOD. It has been shown that oxygen transfer into settling sediment particles is much higher than for settled particles accumulated at the sediment surface. Compared to particles at the SWI, discrete settling particles have a much higher specific surface area and a much thinner diffusive boundary layer (Jorgensen and Revsbech, 1985).

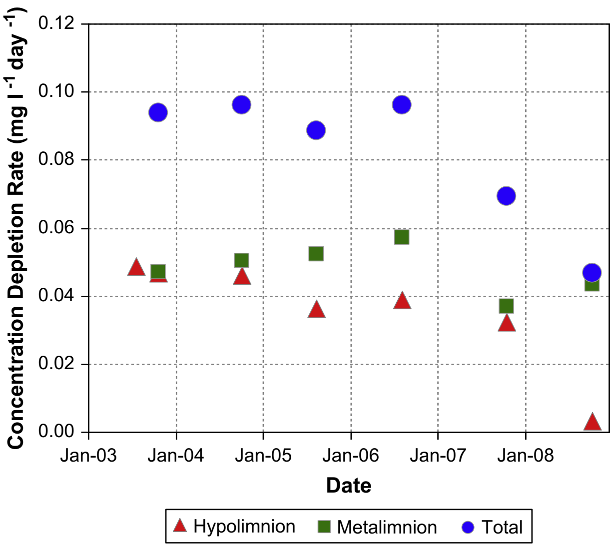

Fig. 8 – Calculated dissolved oxygen concentration depletion rates in Spring Hollow Reservoir. Data for 2003–2006 correspond to background hypolimnion and metalimnion oxygen demand before diffuser was operated. Data for 2007 and 2008 correspond to continuous diffuser operation at 1.3 and 0.61 NCMH, respectively.

3.6. *Long-term reduction of background HOD*

To test the hypothesis that oxygenation over several years may decrease HOD (McQueen and Lean, 1984; Matinvesi, 1996; Moore et al., 1996; Matthews and Effler, 2006a), an analysis of HOD_{conc} and MOD_{conc} was performed during periods when the diffuser was not in operation. Because the low applied gas flow rate was observed to induce negligible oxygen demand (as discussed in Section 3.4), data were also analyzed for periods when the diffuser was in operation (2007–2008). In 2003–2006, HOD_{conc} and MOD_{conc} were calculated based on data collected during similar periods of stratification. In contrast, HOD_{conc} and MOD_{conc} values for 2007 and 2008 (collected between April and October) were calculated as net oxygen demand, which is the difference between measured accumulation in the hypolimnion and the addition rate predicted by the bubble plume. Because the 2003–2006 data represent HOD_{conc} during periods without oxygenation and the 2007 and 2008 data do not include any induced demand, these rates are all equivalent to background HOD_{conc} values. Fig. 8 shows, a decreasing trend in background HOD_{conc} over time.

Several factors may contribute to the observed decrease in HOD_{conc} and MOD_{conc} over time. Variations in hypolimnion volume could theoretically affect oxygen depletion rates because the sediment surface area contributing to SOD is a function of hypolimnion volume. However, hypolimnion volumes were determined and no statistical relationship between HOD_{conc} and hypolimnetic volume was found. Oxygen depletion rates may also be affected by changes in organic loading. Decreased levels of organic matter in the water column would require less oxygen for decomposition, resulting in reduced HOD. However, MOD_{conc} remained relatively constant over time (Fig. 8), which suggests that organic loading also remained relatively constant. It is therefore concluded that the reduction in HOD is caused by a reduction in oxygen consumption processes (e.g., decreasing SOD in subsequent years by more complete organic matter decomposition in the current year).

3.7. Long-term reduction of induced HOD

The decrease in background HOD_{conc} for SHR represents a significant benefit of long-term oxygenation. Because historical data for CCR are not available to verify this observation, the possibility of a decreasing induced HOD_{conc} was investigated. This analysis was performed using data from SHR (2004–2008) and CCR (2006–2007) prior to the onset of the metalimnetic minimum to avoid effective depth influences on induced HOD. Variations in induced HOD_{conc} were tracked as a function of applied gas flow rate. At equivalent gas flow rates, induced HOD_{conc} was observed to decrease over time in both SHR and CCR (data not shown). Furthermore, increasing the gas flow rate during more recent years induced approximately the same HOD_{conc} observed at lower flow rates in previous years. For example, SHR diffuser operation in 2006 at 8.5 and 17 NCMH resulted in similar HOD_{conc} rates in 2005 at flow rates of 3.4 and 8.5 NCMH, respectively. Likewise induced HOD_{conc} values in CCR during 2007 at flow rates of 51 and 85 NCMH were similar to induced HOD_{conc} values during 2006 at flow rates of 34 and 51 NCMH, respectively. These decreases in induced oxygen demand support the results showing long-term decreases in background oxygen demand.

Decreased HOD over time is also revealed in the applied gas flow rates. In SHR, the applied gas flow rate during 2007 was 1.3 NCMH, but was reduced to 0.6 NCMH for 2008. Despite this 50% reduction in oxygen addition rate, the volume-averaged hypolimnion oxygen concentration was much higher in 2008 than in 2007 (see Fig. 7). In CCR, the applied gas flow rate to the diffuser was decreased from 68 NCMH in 2005 to 51 NCMH in 2008 while similar levels of water quality were maintained.

4. Conclusions

Hypolimnetic oxygenation systems were operated in two reservoirs (SHR and CCR) over a wide range of applied gas flow rates. Temperature and oxygen profiles were collected during key experimental periods from 2003 to 2008 to monitor hypolimnetic warming and oxygen depletion rates. A linear-bubble-plume model was used to estimate the rate of oxygen addition to the hypolimnion. Major conclusions are:

1. Accelerated warming was observed in both reservoirs, but was not substantial enough to significantly disrupt thermal stratification. The rate of warming was shown to be a function of the applied gas flow rate, indicating that hypolimnetic warming is a consequence of diffuser-induced mixing.
2. Applied gas flow rate and resulting diffuser-induced mixing were also found to strongly influence HOD. HOD was observed to increase in response to mixing-induced increases in the effective depth of the hypolimnion.
3. HOD was shown to be independent of oxygen concentration in the hypolimnion, indicating that HOD is a zero-order process with respect to oxygen concentration.
4. Although induced mixing was found to increase HOD in the short-term, oxygenation over longer periods of time (several years) appears to decrease background HOD as well as the degree of induced HOD.

In summary, despite increased oxygen demand and warming in the hypolimnion during diffuser operation, the oxygenation systems were able to replenish hypolimnetic oxygen in both CCR and SHR and eventually caused a decrease in both background and diffuser-induced HOD. Hypolimnetic oxygenation remains a viable method for managing source waters in drinking-water-supply reservoirs.

Acknowledgements

We thank Bob Benninger and Gary Robertson of the Western Virginia Water Authority (WVWA) for financial support and the entire WVWA staff for enabling us to work in such a constructive environment. We also thank the two anonymous reviewers for their valuable comments.

REFERENCES

Agusti, S., Duarte, C.M., Kalff, J., 1987. Algal cell size and the maximum density and biomass of phytoplankton. Limnology and Oceanography 32 (4), 983–986.

Ashley, K.I., 1981. Effects of hypolimnetic aeration on functional components of the lake ecosystem. Master of Science Thesis, University of British Columbia.

Ashley, K.I., 1983. Hypolimnetic aeration of a naturally eutrophic lake: physical and chemical effects. Canadian Journal of Fisheries and Aquatic Sciences 40 (9), 1343–1359.

Beutel, M.W., Horne, A.J., 1999. A review of the effects of hypolimnetic oxygenation on lake and reservoir water quality. Lake and Reservoir Management 15 (4), 285–297.

Beutel, M., 2003. Hypolimnetic Anoxia and sediment oxygen demand in California Drinking water reservoirs. Lake and Reservoir Management 19 (3), 208–221.

Beutel, M., Hannoun, I., Pasek, J., Kavanagh, K.B., 2007. Evaluation of hypolimnetic oxygen demand in a large eutrophic raw water reservoir, San Vicente Reservoir, Calif. Journal of Environmental Engineering 133 (2), 130–138.

Burris, V.L., McGinnis, D.F., Little, J.C., 2002. Predicting oxygen transfer and water flow rate in airlift aerators. Water Research 36, 4605–4615.

Cooke, G.D., Welch, E.B., Peterson, S.A., Nichols, S.A., 2005. Restoration and Management of Lakes and Reservoirs. Taylor & Frances Group.

Davis, W.S., Fay, L.A., Herdendorf, C.E., 1987. Overview of USEPA/Clear Lake Erie sediment oxygen demand investigations during 1979. Journal of Great Lakes Research 13 (4), 731–737.

Eckert, W., Imberger, J., Saggio, A., 2002. Biogeochemical response to physical forcing in the water column of a warm monomictic lake. Biogeochemistry 61, 291–307.

Higashino, M., Stefan, H.G., 2005. Sedimentary microbial oxygen demand for laminar flow over a sediment bed of finite length. Water Research 39, 3153–3166.

Jorgensen, B.B., Revsbech, N.P., 1985. Diffusive boundary layers and oxygen uptake of sediments and detritus. Limnology and Oceanography 30 (1), 111–222.

Lorenzen, M.W., Fast, A.W., 1977. A Guide to Aeration/Circulation Techniques for Lake Management. Ecology Research Series EPA-600/3-77-004. US Environmental Protection Agency.

Mackenthun, A.A., Stefan, H.G., 1998. Effect of flow velocity on sediment oxygen demand: experiments. Journal of Environmental Engineering 124 (3), 222–230.

Madigan, M.T., Martinko, J.M., Parker, J., 2003. Brock Biology of Microorganisms, tenth ed. Pearson Education Inc., New Jersey, pp. 115–116,576.

Matinvesi, J., 1996. The change of sediment composition during recovery of two Finnish lakes induced by waste water purification and lake oxygenation. Hydobiologia 335, 193–202.

Matthews, D.A., Effler, S.W., 2006a. Assessment of long-term trends in the oxygen resources of a recovering urban lake, Onondaga Lake, New York. Lake and Reservoir Management 22 (1), 19–32.

Matthews, D.A., Effler, S.W., 2006b. Long-term changes in the areal hypolimnetic oxygen deficit (AHOD) of Onondaga Lake: evidence of sediment feedback. Limnology and Oceanography 51 (1, part 2), 702–714.

McGinnis, D.F., Little, J.C., 2002. Predicting diffused-bubble oxygen transfer rate using the discrete-bubble model. Water Research 36, 4627–4635.

McGinnis, D.F., Lorke, A., Wüest, A., Little, J.C., 2004. Interaction between a bubble plume and the near field in a stratified lake. Water Resources Research 40 (10) citation number W10206.

McQueen, D.J., Lean, D.R.S., 1984. Hypolimnetic aeration: changes in bacterial populations and oxygen demand. Archiv für Hydrobiologie 99 (4), 498–514.

Moore, B.C., Chen, P.H., Funk, W.H., Yonge, D., 1996. A model for predicting lake sediment oxygen demand following hypolimnetic aeration. Water Resources Bulletin 32 (4), 723–731.

Moore, B., 2003. Downflow bubble contact aeration technology (Speece Cone) for sediment oxygenation, remediation of contaminated sediments. In: Proceedings of the Second International Conference on Remediation of Contaminated Sediments, September 30, 2003.

Nakamura, H., Stefan, H.G., 1994. Effect of flow velocity on sediment oxygen demand: theory. Journal of Environmental Engineering 120 (5), 996–1016.

Prepas, E.E., Field, K.M., Murphy, T.P., Johnson, W.L., Burke, J.M., Tonn, W.M., 1997. Introduction to the Amisk Lake Project: oxygenation of a deep, eutrophic lake. Canadian Journal of Fisheries and Aquatic Sciences 54 (9), 2105–2110.

Quinlan, R., Paterson, A.M., Smol, J.P., Douglas, M.S.V., Clark, B.J., 2005. Comparing different methods of calculating volume-weighted hypolimnetic oxygen (VWHO) in lakes. Aquatic Science 67, 97–103.

Rasmussen, H., Jorgensen, B.B., 1992. Microelectrode studies of seasonal oxygen uptake in a coastal sediment: role of molecular diffusion. Marine Ecology Progress Series 81, 289–303.

Singleton, V.L., Little, J.C., 2006. Designing hypolimnetic aeration and oxygenation systems – a review. Environmental Science & Technology 40, 7512–7520.

Singleton, V.L., Gantzer, P., Little, J.C., 2007. Linear bubble plume model for hypolimnetic oxygenation: full-scale validation and sensitivity analysis. Water Resource Research 43 (2), W02405, doi:10.1029/2005WR004836.

Soltero, R.A., Sexton, L.M., Ashley, K.I., McKee, K.O., 1994. Partial and full lift hypolimnetic aeration of Medical Lake, WA to improve water quality. Water Research 28 (11), 2297–2308.

Thomas, J.A., Funk, W.H., Moore, B.C., Budd, W.W., 1994. Short term changes in Newman Lake following hypolimnetic aeration with the Speece Cone. Lake and Reservoir Management 9 (1), 111–113.

Weilenmann, U., O'Melia, C.R., Stumm, W., 1989. Particle transport in lakes: models and measurements. Limnology and Oceanography 34 (1), 1–18.

Wetzel, R.G., 1975. Limnology. W.B. Saunders Company, Philadelphia. 68–71.

Zaw, M., Chiswell, B., 1999. Iron and manganese dynamics in lake water. Water Research 33 (8), 1900–1910.